Extended Abstracts of the Ninth JSME-KSME Thermal and Fluids Engineering Conference
October 28-30, 2017, Okinawa, Japan

TFEC9-1565

NUMERICAL PREDICTION OF AERODYNAMIC SOUND RADIATED FROM VORTICAL FLOW, BASED ON COMPACT GREEN'S FUNCTION

S. Ogawa[1*], M. Hashiguchi[2], K. Yano[1]

[1]National Institute of Technology, Kure College, Kure 737-8506, Japan
[2]Engineering System Co., Ltd, Tokyo 101-0047, Japan

ABSTRACT

There have been so many studies to reveal the generation mechanism of aerodynamic sound produced by longitudinal vortices. The present authors also have so far been investigating mechanism of generation and collapse of a longitudinal vortex system, using a delta wing. However, it has not yet been clarified that how the longitudinal vortex system is generated and how this system produces the aerodynamic sound. The final objective of our study, therefore, is to simplify this specific aerodynamic sound problem to obtain a thorough understanding of how the longitudinal vortex system is produced, and how the noise is generated. Current literatures have numerically predicted dipole sound based on Lighthill-Curle's equation, but have given a little information on the structure of sound sources. As an alternative method, the present paper features Howe's method where the compact Green's function is utilized and related to the cross product of vorticity vector and velocity vector. The study aims to clarify the relationship between unsteady vortical flow and aerodynamically produced sound, combining numerical analyses and the compact Green's function and tries to provide detailed information on the vortices in the flow that most contribute to the generation of sound. As a result, it was found that lift force fluctuations generated by Karman's shedding vortices have good correlation with the aerodynamically produced sound in the far field.

KEYWORDS: Aerodynamic sound, Delta wing, Longitudinal vortices, Compact's Green function

1. INTRODUCTION

The sound induced by turbulence in an unbounded fluid is generally called aerodynamic sound. With respect to aerodynamic sound, Lighthill [1], Curle [2] and Howe [3] [4] have made their theoretical contributions to clarifying the relationship between turbulent flow and sound. In most applications of Lighthill's theory it is necessary to generalize the solution to account for the presence of solid bodies in the flow. Curle [2] has made an extension to Lighthill's general theory of aerodynamic sound so as to incorporate the influence of solid boundaries upon the sound field. The present authors simulated aerodynamic sound generated by the longitudinal vortex using a delta wing based on incompressible flow computation with Lighthill-Curle' equation [5]. Howe recast Lighthill's equation in a form that emphasizes the prominent role of vorticity in the production of sound by taking the total enthalpy as the independent acoustic variable, which leads to the vortex sound equation. These theories have emphasized that unsteady motions of the vortex play a crucial role in the generation of aerodynamic sound. The present authors [6] [7] [8] have studied aerodynamically sound generated by the longitudinal vortex behind the front pillar of an automobile. However, it was found that experiments and numerical analyses based on Lighthill Curle's equation are limited to obtain sufficient information on the structure of sound sources. Therefore the present study tries to reveal the relation between unsteady vortical flows and aerodynamically produced sound by means of the combination of unsteady numerical simulation and the Green's function provided by Howe [3] [4]. Takaishi *et al*. [9] also proposed a new method to evaluate dipole sound sources in a finite computational domain. The study focuses on aerodynamic sound for high Reynolds number flow at low Mach number.

*Corresponding Author:ogawa@kure-nct.ac.jp

2. COMPACT GREEN'S FUNCTION

2.1 Vortex Sound Theory Lighthill first developed the theory of aerodynamic sound by reformulating the Navier-Stokes equation into an exact inhomogeneous wave equation. Howe simplified Lighthill's equation for high Reynolds number flow at low Mach number.

$$\left(\frac{1}{c_0^2}\frac{\partial^2}{\partial t^2}-\nabla^2\right)\left[c_0^2(\rho-\rho_0)\right]=\frac{\partial^2 T_{ij}}{\partial x_i x_j}, \tag{1}$$

and

$$T_{ij}=\rho v_i v_j+\left((p-p_0)-c_0^2(\rho-\rho_0)\right)\delta_{ij}-\sigma_{ij}, \tag{2}$$

where T_{ij} is Lighthill stress tensor, $\rho v_i v_j$; Reynolds stress. Einstein's summation convention is utilized. Howe simplified Lighthill's equation for high Reynolds number flow at low Mach number,

$$\left(\frac{1}{c_0^2}\frac{\partial^2}{\partial t^2}-\nabla^2\right)B=div(\boldsymbol{\omega}\times\boldsymbol{v}), \tag{3}$$

where B is the total enthalpy,

$$B\equiv\frac{p}{\rho_0}+\frac{1}{2}v^2, \tag{4}$$

and $\omega=\nabla\times u$ is the vorticity.
If the observer **x** is far enough from the source region, Green's theory yields the sound pressure at **x**:

$$p_a(\boldsymbol{x},t)=-\int_{\Omega_{all}}(\boldsymbol{\omega}\times\boldsymbol{v})\cdot\nabla G(\boldsymbol{x},\boldsymbol{y},t-\tau)d\boldsymbol{y}d\tau. \tag{5}$$

Here we introduce Y_i which denotes the velocity potential of an imaginary flow around the body that has unit speed in the i direction at large distances from the body.

$$\nabla^2 Y_i=0 \tag{6}$$

In the fluid and also

$$\frac{\partial Y_i(\boldsymbol{y})}{\partial n}=0 \tag{7}$$

on surfaces. Note that the Green's function governs the acoustical properties of the system: the velocity potential Y_i depends on the body shape, but does not represent a real flow. We can express

$$p_a(\boldsymbol{x},t)=-\frac{\rho_0 x_i}{4\pi c_0|\boldsymbol{x}|^2}\int_{\Omega_{all}}\frac{\partial}{\partial t}(\boldsymbol{\omega}\times\boldsymbol{v})(\boldsymbol{y},t-\frac{|\boldsymbol{x}|}{c_0})\cdot\nabla Y_i d\boldsymbol{y}. \tag{8}$$

The force F_i exerted on an incompressible inviscid (or high Reynolds number) fluid flow by a body is generally given as

$$F_i=-\rho_0\int_{\Omega all}(\boldsymbol{\omega}\times\boldsymbol{v})\cdot\nabla Y_i d\boldsymbol{y}=\int_S pn_i dS, \tag{9}$$

where the unit normal vector n_i on S is directed into the fluid domain Ω. By using the relation (9), Equation (8) is reformulated into the form

$$p_a(\boldsymbol{x},t)=\frac{x_i}{4\pi c_0|\boldsymbol{x}|^2}\int_S\frac{\partial}{\partial t}p(\boldsymbol{y},t-\frac{|\boldsymbol{x}|}{c_0})n_i dS, \tag{10}$$

which is identical to the dipole sound term in Curle's equation. If we define another velocity potential φi that would be produced by translational motion of S as a rigid body at unit speed in the i direction, the relationship between Yi and φ_i

$$Y_i=y_i-\varphi_i \tag{11}$$

Finally, the dipole sound is evaluated in the form

$$p_a(\boldsymbol{x},t) = \frac{\rho_0 x_i}{4\pi c_0 |\boldsymbol{x}|^2} \int \frac{\partial}{\partial t}(\boldsymbol{\omega} \times \boldsymbol{v})(\boldsymbol{y}, t - \frac{|\boldsymbol{x}|}{c_0}) \cdot \nabla \varphi_i \, d\boldsymbol{y}. \tag{12}$$

The cross term $\boldsymbol{\omega} \times \boldsymbol{v}$ will be computed, based on unsteady flow computation as described below.

2.2 Compact Green's Function for Circular Cylinder The potentials φ_i φ_I for the circular cylinder of diameter D can be found.

$$Y_i = y_i \,, \qquad \varphi_i = 0 \,. \tag{13}$$

In case of a long cylinder, there exists the following analytical solution

$$\varphi_1 = -\frac{y_1}{y_1^{\,2} + y_2^{\,2}} \left(\frac{D}{2}\right)^2, \qquad \varphi_2 = -\frac{y_2}{y_1^{\,2} + y_2^{\,2}} \left(\frac{D}{2}\right)^2, \qquad \varphi_3 = 0 \,. \tag{14}$$

3. AERODYNAMIC ANALYSIS

3.1 Numerical Method

This study employed time–dependent flow computation to obtain $\boldsymbol{\omega} \times \boldsymbol{v}$ of Eq. (12), based on RANS (Reynolds Averaged Navier-Stokes Simulation). This approach is valid when the maximum Mach number in the domain is less than 0.2–0.3. Eddy viscosity models use the concept of a turbulent viscosity to model the Reynolds stress tensor as a function of mean flow quantities. For the accurate simulation, Menter SST k-ω model was used as the hybrid models in the form that k-ω model was used close to the wall whereas the standard k –ε in the completely turbulent region was employed. The SST k-ω turbulence model is a two-equation eddy-viscosity model which has become very popular. The shear stress transport (SST) formulation combines the best of two worlds. The use of a k-ω formulation in the inner parts of the boundary layer makes the model directly usable all the way down to the wall through the viscous sub-layer, hence the SST k-ω model can be used as a Low Re turbulence model without any extra damping functions. The SST formulation also switches to a k-ε behavior in the free-stream and thereby avoids the common k-ω problem that the model is too sensitive to the inlet free-stream turbulence properties. It therefore follows that SST k-ω model often merit it for its good behavior in adverse pressure gradients and separating flow. In the steady state analysis, the maximum step number is 3,500. Reynolds number is defined in Equation (1), where mean air flow velocity U= 20 m/s, D = 0.01m and cylinder length L = 4.8D = 0.048 m and kinematic viscosity ν=1.476×10^{-6} m^2/s and results in Re = 1.4×10^4. It therefore follows that the analyses were conducted for high Reynolds number flow at low Mach number (0.059). Figures 1 and 2 shows the total computational domain and the prism layer mesh model close to the surface of the circular cylinder. This layer of cells is necessary to improve the accuracy of the flow solution. The prism layer mesh is defined in terms of its thickness, the number of cell layers, and the size distribution of the layers. In this study the thickness of prism layer is 0.25 mm and the number of cell layer is 5 and mesh size is 0.06 mm closest to the model surface. Total cell numbers amount to 11,400,000.

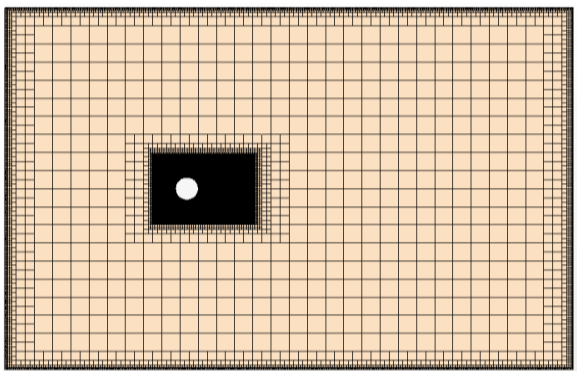

Fig. 1 Computational domain.

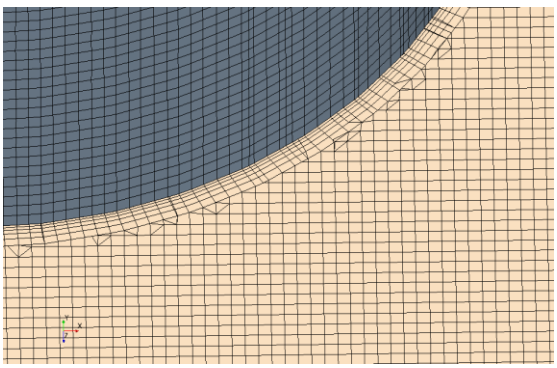

Fig. 2 Mesh in the vicinity of circular cylinder.

3.2 Results and Discussion Figure 3 shows the prediction of lift coefficient fluctuations. The lift fluctuations are analyzed by FFT analysis as shown in Fig. 4. Peak frequency can be observed at about 150 Hz. Flow patterns around the cylinder were also captured as in Figs. 5 and 6. Figure 7 shows the vorticity behind the cylinder. It is found that Karman vortices are being shed regularly, which exerts the influence of vortex shedding on pressure fluctuations on the surface of the cylinder. The sound pressure level calculated based on pressure fluctuations as shown in Fig. 8. The measuring point is 0.1 m away from the cylinder at the center in the Z direction. Peak frequency is about 150 Hz which is almost the same as that of unsteady lift forces shown in Fig. 4.

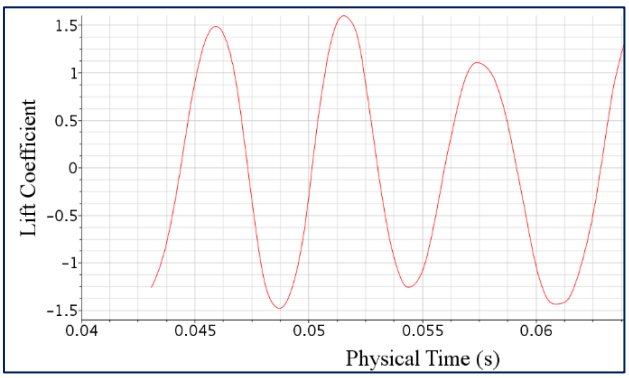

Fig. 3 Lift fluctuations.

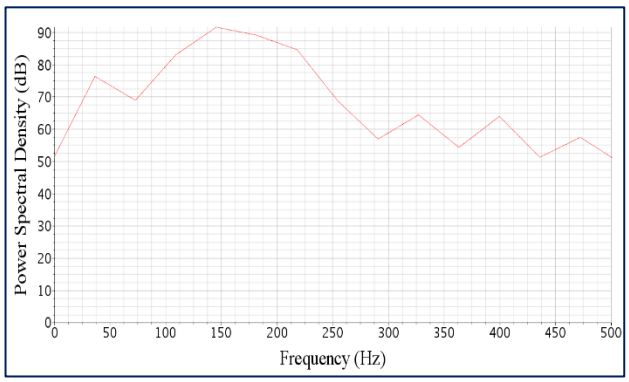

Fig. 4 FFT analysis of Lift fluctuations.

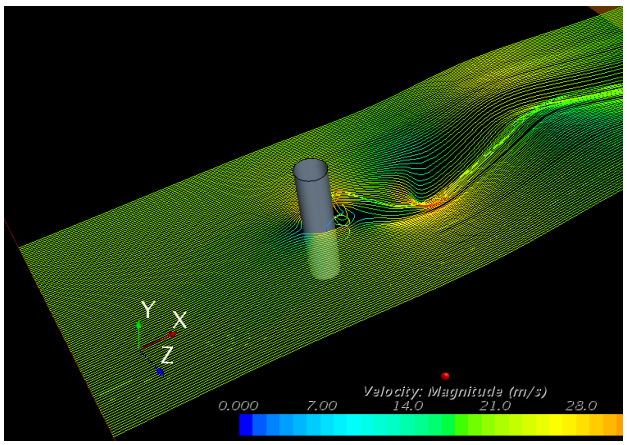

Fig. 5 Streamlines around the cylinder.

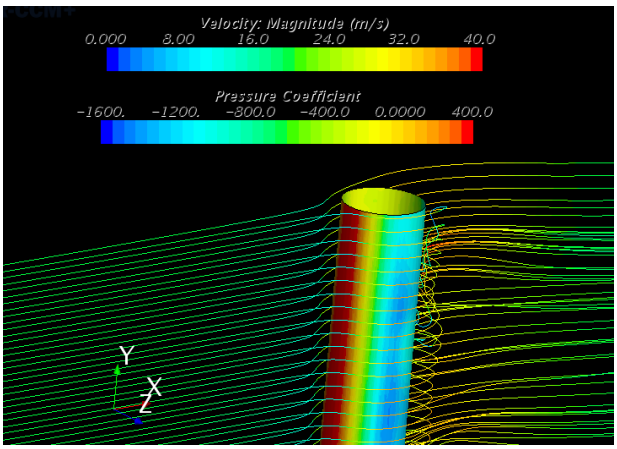

Fig. 6 Streamline and pressure on the cylinder.

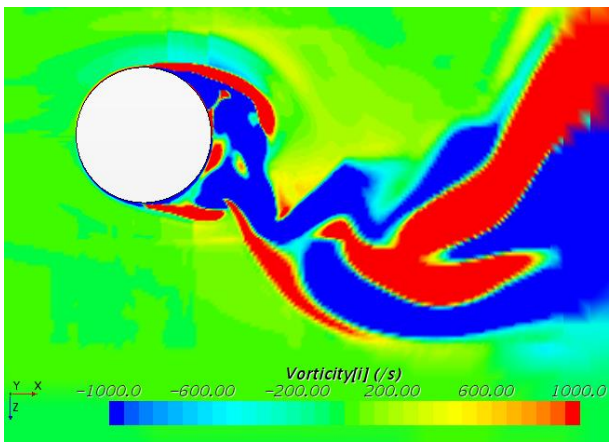

Fig. 7 Vorticity behind the cylinder.

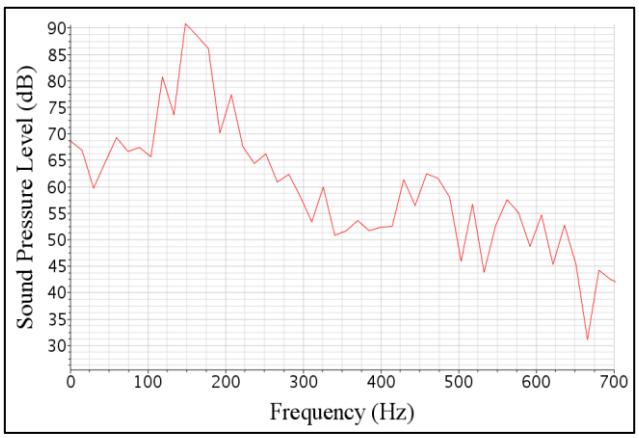

Fig. 8 Sound pressure level at 0.1 m from the cylinder.

4. CONCLUSION

Howe's method is basically equivalent to Lighthill-Curle's one. Since this method can directly relate the structure of flow field to the sound sources, it is considered that we can improve the configuration of an object, seeing flow patterns around it. On the other hand, in case of Lighthill-Curle's method we are required to measure pressure fluctuations on the object at the multipoint simultaneously, but it is substantially difficult to measure them.

From a numerical result, it is found that the peak frequency of the unsteady lift forces coincide with that of aerodynamic sound in the far field.

REFERENCES

[1] Lighthill, M.J., "On sound generated aerodynamically I. general theory," *Proc. R. Soc. London A, 211*, 564-587. http://rspa.royalsocietypublishing.org/content/211/1107/564, (1952).

[2] Curle, N., "The influence of solid boundaries upon aerodynamic sound," *Proc. R. Soc. London A, 231*, 505-514. http://rspa.royalsocietypublishing.org/content/231/1187/505.short, (1955).

[3] Howe, M.S. *Theory of vortex sound*: Cambridge Texts in Applied Mathematics, Cambridge University Press, pp.41-61(2003).

[4] Howe, M.S. *Acoustics and aerodynamic sound*, Cambridge University Press, pp. 47-100 (2014).

[5] Ogawa, S., Hashiguchi, M., Kamimoto, I., Kuwahara, K., "Numerical study of aerodynamic noise radiated from a three-dimensional wing," *SAE*, Vol.101 920205(1992).

[6] Ogawa, S., Li, Y., "Control of longitudinal vortex generated around front pillar of vehicles, based on clarification of the vortex generation mechanism using a delta wing," *Proceedings of the 12th International Conference on Motion and Vibration Control*, 1-16 (2014).

[7] Ogawa, S., Takeda, J., "Mechanism of Generation and Collapse of a Longitudinal Vortex System Induced around the Leading edge of a delta wing," *Open Journal of Fluid Dynamics*, Vol.5, 265-274 (2015).

[8] Ogawa, S., Kawate, T., Takeda, J., Yano, K., "Aerodynamic sound radiated from longitudinal and transverse vortex systems generated around the leading edge of delta wings," *Open Journal of Fluid Dynamics*,Vol.6, 101-118 (2016).

[9] Takaishi, T., Ikeda M., Kato C., "Method of evaluating dipole sound source in a finite computational domain," J. Acoustic Soc. Am. 116 (3), 1427-1435 (2004).